

Mass Transfer Rates in Ion Exchange

W. A. SELKE, Y. BARD, A. D. PASTERNAK, and S. K. ADITYA

Columbia University, New York, New York

The rates of both the liquid-phase mass transfer and the internal-diffusion steps in ion exchange were studied by means of shallow-bed experiments. The mass transfer coefficients obtained fitted the general correlations for other packed-bed operations when the Schmidt group was evaluated with experimentally determined ionic counterdiffusivities. An incremental calculation of the diffusion rates within the particles yielded a value of the counterdiffusivity in the resin phase. A general design procedure based on these findings is proposed.

The integration of mass transfer data for ion exchange columns with the correlations for other unit operations using packed beds has been hindered by the complexity of the rate mechanism of ion exchange, by the paucity of appropriate diffusivity data, and by the difficulties encountered in the mathematical treatment of cyclical fixed beds.

Over a wide range of conditions the rate of ion exchange has been shown to be governed by a combination of liquid-phase mass transfer and internal diffusion steps. Because of the transient nature of the diffusion in the particles it cannot be represented rigorously by an ordinary differential equation with constant rate coefficients. Over-all coefficients, which are convenient in those operations in which the mass transfer in both phases can be regarded at any instant as taking place at steady state, are not even approximately constant with time when one phase is immobile (12). Although simplified rate expressions can be useful expedients and are required for simple design procedures, they do not give suitable indication of the importance of each rate step when employed for the analysis of data.

Most experimental studies of ion exchange rates have been on fixed beds (7, 13). In order to extract rate information from the data, it is necessary to relate the effluent concentration history to the rate coefficient. Formal solutions for the fixed bed with a number of special cases of equilibrium and rate mechanism have appeared, but few experimental systems conform exactly to the models represented by the equations. The only work treating rigorously the important combined liquid and internal-resistance rate mechanism is that of Rosen (11) for linear equilibrium.

In most previous studies of ion exchange the mass transfer coefficients have been evaluated by the use of certain mathematical simplifications, some of considerable ingenuity (7, 15). The results obtained in this manner were

internally consistent, but perforce of a somewhat empirical nature.

A somewhat more general, though less elegant, approach is the use of shallow-bed experiments for primary rate determinations. This technique permits direct evaluation of instantaneous values of both the liquid- and resin-phase diffusion resistances (2). It is the purpose of this paper to demonstrate that mass transfer coefficients determined in this manner are in accord with the general correlations for packed beds if the Schmidt number is evaluated with the proper diffusivities for the counterflow of ions. The analysis of the internal-diffusion step from shallow-bed data can yield values of the diffusivities for the counterdiffusion inside the resin particles and also point the way to design methods for deep beds.

LIQUID-PHASE MASS TRANSFER COEFFICIENTS

Experimental

Shallow-bed Runs. The exchange of copper for hydrogen ions on Amberlite IR-120, a sulfonated polystyrene bead-form resin, was studied. The resin particles, from a closely sized cut of 0.5 mm. average diameter, were packed in a shallow bed, i.e., in a bed small enough so that average concentrations may be used in mass transfer and material-balance equations without serious error. A copper sulfate solution was fed through the bed at a fixed rate, measured by means of a rotameter. Two kinds of runs were made.

1. Step-input runs, in which an approximately 0.05*N* copper sulfate solution was fed directly to the shallow bed (initially in the hydrogen form). Under these conditions the shallow bed operates similarly to a differential section at the entrance of a deep-bed ion exchanger.

2. Double-bed runs, in which the copper sulfate solution is passed through a deep-bed ion exchanger (initially also in the hydrogen form), prior to being fed to the shallow bed. In this way the shallow bed simulates the operation of a differential section of a deep bed somewhat removed from the entrance section.

Samples from both feed and effluent streams were analyzed photometrically for copper, with tetraethylene-pentamine used as an indicator (4).

Ionic Counterdiffusivities. Measurements

were made by means of a cell consisting of two chambers separated by a sintered-glass membrane. One of the chambers was filled with a copper sulfate solution of the same concentration (approximately 0.05*N*) as was used in the shallow-bed runs, and the other one with a sulfuric acid solution of exactly the same normality. Thus copper and hydrogen ions would counterdiffuse through the membrane, approximating conditions in the liquid phase during an ion exchange operation. The cell was placed in a thermostat held at 25°C., a temperature close to that of the shallow-bed runs. At the end of a measured period of contact the solutions in both chambers were analyzed for copper ion concentration and the diffusivity was determined from the formula

$$\ln \Delta c_0 / \Delta c = \beta D t$$

where Δc_0 and Δc are the differences between the copper ion concentrations in the two chambers at the beginning and at time t respectively, D the diffusivity, and β a cell constant, determined by means of a run with a system of known diffusivity (KCl into pure H_2O). The foregoing formula assumes no concentration gradients in the bulk of the solution in each chamber (8).

The counterdiffusivity of silver and hydrogen ions was determined in similar fashion by use of equinormal silver nitrate and nitric acid solutions.

Results

It has been shown (2, 9) how the results of shallow-bed runs can be interpreted to give concentrations in the liquid and resin phases, as well as at the interface, and $K_L S$ as functions of time, as well as the value of $k_L S^*$, the latter two quantities being defined by Equation (1):

$$\begin{aligned} \frac{dq}{dt} &= k_L S(C - C_i) \\ &= K_L S(C - C^*) \end{aligned} \quad (1)$$

In Table 1 are listed the operating conditions and the values of $k_L S$ for the runs made by the authors, as well as some obtained from other sources (2), and in Table 2 are the measured counterdiffusivities.

Correlation of Data

General correlations of liquid side coefficients for mass transfer between the

* $k_L S$ is obtained by extrapolation of $K_L S$ to $t = 0$. It was found impossible to do this in the double-bed runs because the values of $K_L S$ for the initial period of the run (until the resin reached about 15% of saturation) showed too much scatter. Step-input runs were therefore made at the same liquid velocity as each double-bed run, and $k_L S$ was obtained from the smooth plot of $K_L S$ vs. t for the step-input runs. These step-input runs are not listed separately in Table 1.

W. A. Selke is with Peter J. Schweitzer, Inc., Lee, Massachusetts.

TABLE 1

Run	System	d_p , cm.	V , cc./sec.	A , sq. cm.	$k_L S$, cc./(g.) (sec.)	Re	j
A2	Cu—H	0.050	0.545	1.98	1.06	4.34	0.723
A3	Cu—H	0.050	0.967	1.98	1.44	7.80	0.556
P1	Cu—H	0.050	0.506	1.00	1.32	8.04	0.491
P2	Cu—H	0.050	0.680	1.00	1.28	10.8	0.353
P3	Cu—H	0.050	0.595	1.00	1.34	9.43	0.426
P4*	Cu—H	0.050	0.541	1.00	1.92	8.60	0.670
P5	Cu—H	0.050	0.326	1.00	1.50	5.20	0.869
P6*	Cu—H	0.050	0.903	1.00	2.25	14.3	0.475
P7	Cu—H	0.050	0.173	1.00	0.945	2.74	1.03
P8*	Cu—H	0.050	0.196	1.00	0.973	3.12	0.934
B1†	Ag—H	0.060	1.38	0.865	2.88	30.3	0.258
B3	Ag—H	0.060	3.17	0.865	4.45	69.4	0.174
B7	Ag—H	0.060	1.81	0.968	2.36	35.6	0.180
B9	Ag—H	0.060	1.76	0.968	2.54	34.4	0.200
B10	Ag—H	0.085	1.28	0.968	1.85	35.6	0.234
B11	Ag—H	0.085	1.16	0.968	1.65	32.2	0.280
B12	Ag—H	0.042	1.17	0.968	3.08	16.3	0.258
B13	Ag—H	0.060	1.23	0.968	2.02	24.1	0.314
B14	Ag—H	0.060	6.31	0.968	4.72	124	0.104
B15	Ag—H	0.060	3.26	0.968	3.55	64.0	0.151
B16	Ag—H	0.060	1.94	0.968	2.55	38.1	0.182

*Double-bed runs.

†Data for runs B1–B16 were taken from reference 1.

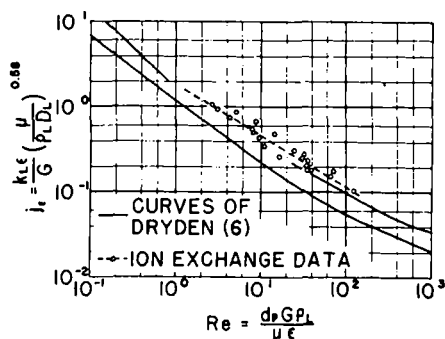


Fig. 1. Correlation of liquid-side mass transfer coefficient.

liquid and a dispersed phase have been prepared by several authors. The following discussion will be based on the correlation presented by Dryden et al. (6). They found that the j_L factor, as defined by Equation (2) can be plotted as a single-valued function of a modified Reynolds number, defined in Equation (3):

$$j_L = \frac{k_L \epsilon}{G} \left(\frac{\mu}{\rho_L D_L} \right)^{0.58} \quad (2)$$

$$Re = \frac{d_p G \rho_L}{\mu \epsilon} \quad (3)$$

It is observed that $k_L/G = (k_L S/S)/(V/A)$ and that for spherical particles

$$S = \frac{4\pi r^2}{4\pi r^3 \rho_s / 3} = \frac{3}{r \rho_s} = \frac{6}{d_p \rho_s}$$

hence

$$j_L = \frac{k_L S \epsilon \rho_s d_p A}{6V} \left(\frac{\mu}{\rho_L D_L} \right)^{0.58} \quad (2a)$$

In the evaluation of these quantities, the following values were used: $\rho_L = 1.00$

*Dryden et al. use k'_L —moles/(hr.) (sq. cm.) (moles/moles), and G_m —moles/(hr.) (sq. cm.) instead of k_L and G as defined here. Their ratio is clearly the same.

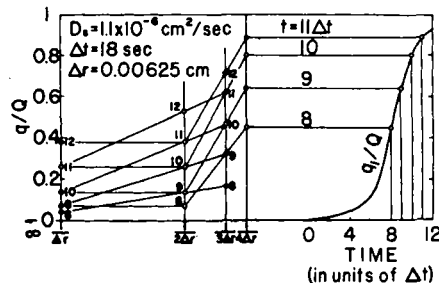


Fig. 2. Sample construction by Schmidt method. (Only a few stages are shown to avoid crowding.)

TABLE 2. MEASURED COUNTERDIFFUSIVITIES

System	D_L , sq. cm./sec. at 25°C.
Cu ⁺⁺ —H ⁺	0.80×10^{-5}
Ag ⁺ —H ⁺	1.74×10^{-5}

g./cc.; $\rho_s = 1.1$ g./cc.; $\mu = 0.009$ g./cc.; $\epsilon = 0.35$.

Values of j_L and Re are listed in Table 1 and plotted in Figure 1, together with the curves from Figure 3 of Dryden et al. (6). It can be seen that the data for ion exchange fall on a smooth curve with the upper of the two curves shown by Dryden.

Although the fit of the data with the correlation is adequate, the effect of changing the values of the constants used is of interest.

Baddour (1) has pointed out that evaluating coefficients for the counterdiffusion of dissimilar ions by observing the motion of only one of these ions can lead to significant error. He estimated that the effective counterdiffusivity for copper-hydrogen ion exchange may be as much as double the value obtained in this work. Substitution of such higher values of D_L in the Schmidt number would bring the ion exchange data to a point midway between the two curves of Dryden on Figure 1.

RESIN-PHASE DIFFUSION

Resin-phase-diffusion studies were made of the system Cu⁺⁺ ion diffusing into the hydrogen form of Amberlite IR-120. The internal diffusivity, D_s , may be defined by Fick's law in polar form:

$$\frac{\partial q}{\partial t} = D_s \left(\frac{\partial^2 q}{\partial r^2} + \frac{2}{r} \frac{\partial q}{\partial r} \right) \quad (4)$$

Incremental Calculation Method

From the data obtained from the double-bed runs (P4, P6, and P8, Table 1), q_i/Q curves were plotted for the shallow bed. These form boundary conditions for Equation (4). In attempting to solve the equation, one assumed that the resin particles are spherical, that concentrations in the particle are functions of time and distance from the center alone, and that D_s does not vary significantly with q and C_0 .

A graphical technique for solving Equation (4) under the foregoing assumptions is available. This is the Schmidt

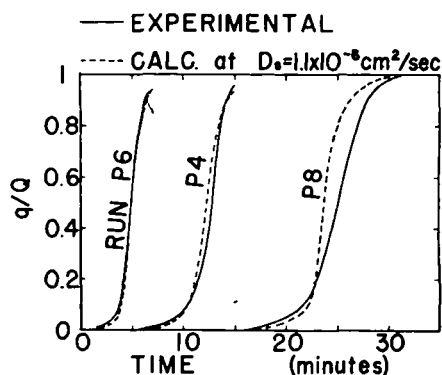


Fig. 3. Resin saturation; comparison of experimental and calculated curves.

method (14), a technique which, with the trial-and-error approach as outlined below, was used to determine the diffusivity, D_s .

A value of D_s was selected. Values were then selected for an increment of radius Δr and an increment of time Δt . The values were chosen so that $D_s \Delta t / \Delta r^2 = 0.5$. Values of $1/n\Delta r$ were plotted as abscissae for $n = 1, 2, 3, \dots, m$, where $m\Delta r$ = the radius of the particle. The values of q_i/Q at the time intervals Δt were plotted as ordinates at the abscissa $1/m\Delta r$. The concentration values at $1\Delta r, 2\Delta r, \dots$, etc., were determined by graphical construction. The Schmidt method is based on the fact that the tie line which connects points representing the concentrations at $r = n\Delta r$ and $(n+2)\Delta r$ at time t crosses the point which represents the concentration at $r = (n+1)\Delta r$ at time $(t + \Delta t)$. See Figure 2 for a sample construction.

The values of q/Q thus obtained at any time t were averaged over the whole particle to obtain $(q/Q)_{avg}$ at any time. These were plotted and compared with the experimental curve. The procedure

was repeated for different values of D_s , until a good check was obtained.

The question arose as to how small Δr must be to assure reasonable accuracy. This was answered by plotting predicted q/Q curves obtained by letting $m = 4$ and $m = 8$. The difference between the two curves was negligible.

Results of Calculation

The resin-phase diffusivity, D_s , was evaluated at three different flow rates at room temperature. The same value $D_s = 1.1 \times 10^{-6}$ sq. cm./sec. was obtained for the three runs analyzed. The agreement between predicted and experimental values of q_i/Q was good (see Figure 3.)

This result may be compared with the findings of Boyd and Soldano (3), who studied the self-diffusivity of many ions in various ion exchange resins to determine the variation of D_s with temperature and with divinyl benzene content, DVB, in the resin. One ion they did not study was Cu^{++} . However, Zn^{++} was studied, and since the atomic weights of zinc and copper are very close and their valences are the same, a comparison will be useful.

Self-diffusion coefficients

Commercial Dowex-50 (5.20 meq./g. dry hydrogen-form)

0.3°C. 25°C.

Zn^{++} : 8.77×10^{-9} 2.89×10^{-8}
sq. cm./sec.

Nominal 24% DVB (4.36 meq./g. dry hydrogen-form)

Zn^{++} : 5.52×10^{-10} 2.63×10^{-9}

Nominal 1% DVB

Zn^{++} 1.06×10^{-6}

Present results—Counterdiffusion coefficient

Amberlite IR-120, 8 to 10% DVB

$\text{Cu}^{++}-\text{H}^+$ 1.1×10^{-6}

The counterdiffusivity for the copper-hydrogen system is apparently increased over the corresponding self-diffusion coefficient for the metal ion by the mobility of the hydrogen ion (1).

It is of interest to compare the ratio of the diffusivities in the solid and liquid phases with values reported in the literature. The experimental values for this case were in the ratio of 7.3:1. This is of the same order of magnitude as measured by Piret, et al. (11) for nonadsorbent-type pore diffusion and one-tenth of the values measured by Dryden and Kay (5) for liquid-phase diffusion into adsorbent carbon pores.

APPLICATION

The results presented here are general and can be applied to the design of ion exchange contactors operating under con-

ditions far removed from the range of experimental conditions. The data required for a design calculation are the equilibrium curve, the internal diffusivity, and the Schmidt number for the ionic system and concentration in question. The equilibrium curve is best determined experimentally (12), although significant progress is being made in the prediction of this curve from available values of physical chemical properties. Both the internal diffusivity and the Schmidt number can be evaluated by a single shallow-bed experiment. The general correlations can then provide mass transfer coefficients for either packed beds or fluidized beds.

As the use of ion exchange is extended to larger units, and to ionic systems for which little empirical knowledge exists, the use of extensive design calculations is increasingly justified. The same techniques used for the analysis of the shallow-bed data can be applied to design. The complete bed can be regarded as a combination of shallow beds. This calculation, tedious if done by hand, can easily be performed by programmed computing machines and can overcome the lack of formal mathematical solutions for the general cases of ion exchange beds. The following is a brief outline of the suggested method of calculation:

1. Divide the deep bed into a suitable number of shallow beds.

2. Assume a curve of surface concentration \bar{q}_i as a function of time for the topmost shallow bed.

3. Calculate q and dq/dt as functions of time by the Schmidt method.

4. Compute the outlet concentration in the liquid phase by means of the material balance

$$V(C_{in} - C_{out}) = W dq/dt$$

where W is the weight of the resin in the shallow bed.

5. Compute $C_{avg} = (C_{in} + C_{out})/2$

6. Obtain the value of $k_L S$ from the generalized correlation.

7. Compute the interfacial concentration in the liquid phase from

$$dq/dt = k_L S(C_{avg} - C_i)$$

8. Obtain from the equilibrium curve the resin-phase interfacial concentration q_i^* that would be in equilibrium with the computed values of C_i and check against the assumed values \bar{q}_i . If the two are not equal, repeat steps 2 to 8 using as the assumed values the average between \bar{q}_i and q_i^* , until agreement is obtained.

9. Repeat steps 2 to 8 for successive sections of the deep bed, using C_{out} from the preceding section as the new C_{in} .

Note that the time scale used in the foregoing calculations must be adjusted from one section to another by subtracting at each point the amount of time that is required for the liquid stream to reach the section in question.

ACKNOWLEDGMENT

The authors wish to acknowledge the financial assistance of the United States Atomic Energy Commission under contract AT(30-1)1108 and the helpful suggestions of Professor C. E. Dryden of Ohio State University.

NOTATION

A = cross-sectional area of bed, sq. cm.
 C = concentration of exchanging ion in liquid, meq./cc.
 d_p = resin particle diameter, cm.
 D = diffusivity, sq. cm./sec.
 G = superficial liquid velocity, cm./sec.
 k = mass transfer coefficient, meq./
(sec.)(sq. cm.)(meq./cc.)
 K = over-all mass transfer coefficient,
meq./
(sec.)(sq. cm.)(meq./cc.)
 q = concentration of exchanging ion in
resin, meq./g.
 Q = exchange capacity of resin, meq./g.
 r = resin-particle radius, cm.
 S = specific surface area of resin, sq. cm./
g.
 t = time, sec.
 V = volumetric rate of flow, cc./sec.
 ϵ = void fraction, cc. void space/cc.
bed volume
 μ = viscosity, g./
(cm.)(sec.)
 ρ = density, g./cc.

Subscripts

i = solid-liquid interface
 L = liquid phase
 S = solid (resin) phase

LITERATURE CITED

1. Baddour, R. F., personal communication.
2. Bieber, Herman, F. E. Steidler, and W. A. Selke, *Chem. Eng. Progr. Symposium Ser. No. 14*, 50, 17 (1954).
3. Boyd, G. E., and B. A. Soldano, *J. Am. Chem. Soc.*, **75**, 6091 (1953).
4. Crumpler, R. B., *Anal. Chem.*, **44**, 2187 (1952).
5. Dryden, C. E., and W. B. Kay, *Ind. Eng. Chem.*, **46**, 2294 (1954).
6. Dryden, C. E., D. A. Strang, and A. E. Withrow, *Chem. Eng. Progr.*, **49**, 191 (1953).
7. Gilliland, E. R., and R. F. Baddour, *Ind. Eng. Chem.*, **45**, 330 (1953).
8. Jost, W., "Diffusion in Solids, Liquids and Gases," pp. 443ff., Academic Press, Inc., New York (1952).
9. Muendel, C. H., and W. A. Selke, *Ind. Eng. Chem.*, **47**, 374 (1955).
10. Piret, E. L., R. A. Ebel, C. T. Kiang, and W. P. Armstrong, *Chem. Eng. Progr.*, **47**, 405 (1951).
11. Rosen, J. B., *Ind. Eng. Chem.*, **46**, 1530 (1954).
12. Selke, W. A., in "Ion Exchange Technology," ed. by F. C. Nachod and J. Schubert, pp. 66ff., Academic Press, Inc., New York (1956).
13. ———, and Harding Bliss, *Chem. Eng. Progr.*, **46**, 509 (1950).
14. Schmidt, E., *Forsch. Gebiete Ingenieurw.*, **13**, 177 (1942).
15. Vermeulen, Theodore, and N. K. Hiester, *Ind. Eng. Chem.*, **44**, 636 (1952).